# Prevalence of the sling effect for enhancing collision rates in turbulent suspensions

Michel Voßkuhle, Alain Pumir, Emmanuel Lévêque
*Laboratoire de Physique, Ecole Normale Supérieure de Lyon, CNRS, Université de Lyon, F-69007, Lyon, France*

Michael Wilkinson
*Department of Mathematics and Statistics, The Open University, Walton Hall, Milton Keynes, MK7 6AA, England*

Turbulence facilitates collisions between particles suspended in a turbulent flow. Two effects have been proposed which can enhance the collision rate at high turbulence intensities: 'preferential concentration' (a clustering phenomenon) and the 'sling effect' (arising from the formation of caustic folds in the phase-space of the suspended particles). We have determined numerically the collision rate of small heavy particles as a function of their size and densities. The dependence on particle densities reveals that the enhancement by turbulence of the collision rate of particles with significant inertia is due almost entirely to the sling effect.

PACS numbers: 47.27.-i, 05.40.-a, 45.50.Tn, 92.60.Mt

Understanding the rate of collisions between small particles, suspended in a turbulent fluid, is necessary for describing a variety of important physical processes. In the case of clouds, collisions between droplets may determine the onset of rainfall [1]. Models for planet formation involve aggregation through collisions of dust grains in the circumstellar disc [2]. Last, collisions between suspended particles may be an important contribution to dissipation of energy in some particle laden flows [3]. It is, therefore, of considerable importance to quantify collisions between particles suspended in a turbulent gas.

The topic of collisions of particles suspended in a turbulent flow has a long history, starting from the seminal work by Saffman and Turner, who were interested in understanding rain initiation in turbulent clouds [4]. Important theoretical insights have emerged in recent years, which indicate that the results of [4] lead to an underprediction of the collision rate when the turbulence intensity is high, as a result of two different mechanisms. First, it has been shown that particles can cluster due to an effect termed 'preferential concentration', which is ascribed to (heavy) particles being expelled from vortices by a centrifugal effect [5] (other interpretations are considered in [6]). This clustering effect can enhance the collision rate. Second, it has been recognized that particles with inertia, which do *not* exactly follow the fluid motion, can both be arbitrarily close, and yet have very different velocities. This effect induces collisions which may be thought as resulting from particles being 'slung' by vortices [7]. This phenomenon can also be understood in terms of caustics in the phase-space of the suspended particles [8, 9]. When the turbulence intensity is sufficiently high, a gas-kinetic model can be used to describe the trajectories [10], sometimes referred to as 'random uncorrelated motion' [11].

These mechanisms for enhancement of the collision rate have been illustrated by simulations on model flows [11, 12]. There have also been investigations of the collision rates in simulations of fully-developed turbulence, which have provided quantitative information on preferential concentration and on the increase of the collision velocity [13–15]. In this paper we report direct numerical simulation (DNS) studies of the collision rate of particles in fully-developed three-dimensional turbulence, as a function of both their size and density. This extended parameter space allows us to separate the clustering and the caustics/sling effect. We find that the caustics/sling effect is the dominant mechanism leading to the enhanced collision rate in turbulent flows, even when the effect of particle inertia is expected to be relatively weak.

In the following paragraphs we discuss the clustering and sling/caustics models for the collision rate, before considering how these compare with our numerical results. We consider a monodisperse suspension of spherical particles, of radius $a$, made of material with density $\rho_{\rm p}$, suspended in an incompressible fluid of density $\rho_{\rm f}$ and kinematic viscosity $\nu$. The fluid, with velocity field $\boldsymbol{u}(\boldsymbol{r},t)$, is in a statistically steady state of turbulent motion with rate of dissipation per unit mass equal to $\epsilon$. We consider a sufficiently dilute suspension, so the flow is not significantly perturbed by the presence of the particles. We assume that the particles obey the simple equation of motion [16, 17]:

$$\dot{\boldsymbol{r}} = \boldsymbol{v} \ , \quad \dot{\boldsymbol{v}} = \frac{1}{\tau_{\rm p}}[\boldsymbol{u}(\boldsymbol{r},t) - \boldsymbol{v}] \tag{1}$$

where

$$\tau_{\rm p} = \frac{2}{9}\frac{a^2}{\nu}\frac{\rho_{\rm p}}{\rho_{\rm f}} \tag{2}$$

is the particle relaxation time, determined from Stokes formula for the drag on a moving sphere. This equation of motion is valid in the limit where the suspended particles are very small and very dense: $\rho_{\rm p}/\rho_{\rm f} \gg 1$.

In determining the motion of particles by using (1), only one parameter is needed, namely the relaxation time $\tau_{\rm p}$. This time scale should be compared to a time scale of

the flow. To this end, we introduce the Stokes number, as the ratio between $\tau_{\rm p}$ and the characteristic time of the flow at the smallest scale, the Kolmogorov time scale $\tau_{\rm K} \equiv (\nu/\epsilon)^{1/2}$:

$$\mathrm{St} = \frac{\tau_{\rm p}}{\tau_{\rm K}} \ . \tag{3}$$

The Stokes number parametrizes the effect of particle inertia. For $\mathrm{St} \ll 1$, particles are advected by the fluid, and collisions are the result of shear. When $\mathrm{St} \gg 1$, the inertia of the particles allows them to move relative to the surrounding fluid. Note that $\mathrm{St} \propto \sqrt{\epsilon}$, so that the inertial effects become more important when the turbulent intensity increases. In the range of droplet size most relevant in the cloud microphysics context, $10\mu\mathrm{m} \lesssim a \lesssim 20\mu\mathrm{m}$, the Stokes number reaches at most values of the order of $\mathrm{St} \sim 0.3$ [18]. In other applications, such as planet formation [19], very large Stokes numbers are relevant.

We count a collision as occuring when the separation of the centers of independently moving particles come within $2a$. The collision rate $R$, defined as the probability per unit time for a given particle to collide with any of the other particles, is proportional to the volume density of the other particles, $n_0$, to the cross sectional area ($\propto a^2$) and to some appropriate average of the relative velocity for colliding particles, denoted by $\langle w \rangle$:

$$R = 4\pi n_0 (2a)^2 \langle w \rangle \ . \tag{4}$$

The expected total number of collisions in a closed system of volume $V$ is simply obtained by multiplying $R$ by $n_0 V/2$. We neglected the role of gravity, and of hydrodynamic interactions which may inhibit collisions by trapping a lubricating layer between the particles. We are concerned here with the collision rate for this slightly simplified model. The objective is to describe the collision rate determined from our DNS studies within the framework of a parametrisation based upon recent theoretical insights.

In the limit $\mathrm{St} \ll 1$ the collision rate is determined by shearing motion, so that $\langle w \rangle \sim (2a)/\tau_{\rm K}$. Saffman and Turner argued that

$$R_{\rm ST} = \sqrt{\frac{8\pi}{15}} \frac{n_0 (2a)^3}{\tau_{\rm K}} \ . \tag{5}$$

Their calculation includes all instances in which the separation radius decreases past $2a$. In the case of collisions where particles stick or coalesce on contact, we should only count the first contact collisions. This effect should be accounted for by introducing a factor $f < 1$ in (5). We ignore these corrections which will be discussed in a future publication, and simply set $f = 1$ here.

The enhancement of the collision rate, compared to the prediction of (5), is expected to come from the particle trajectories breaking away from the fluid as the Stokes number increases. The effect termed preferential concentration causes clustering of particles with finite values of St. The density of particles at a distance $r$ from a given test particle is $n_0 g(r)$, where $g(r)$ is a radial correlation function. The relative velocity is not affected by the preferential concentration effect, so the collision rate due to particles being advected into contact by shearing motion is

$$R_{\rm adv} = \sqrt{\frac{8\pi}{15}} \frac{n_0 (2a)^3}{\tau_{\rm K}} g(2a) \ . \tag{6}$$

At a fixed Stokes number, the function $g(r)$ has a power-law dependence upon $r$: $g(r) \propto r^{\zeta}$ [20]. This reflects the expectation that the suspended particles should sample a fractal measure [21, 22]. The exponent is $\zeta = d - D_2$, where $D_2$ is the correlation dimension [23]. DNS results indicate that for three dimensional turbulent flows, $2.3 \leq D_2 \leq 3$ [24].

In the limiting case where the turbulence intensity is very high, an alternative approach to understanding the effect of increasing the turbulence intensity was initiated by Abrahamson [10] , who pointed out that a gas-kinetic approach can be used to model the motion of the suspended particles. In this limit the relative velocity due to shearing motion induced by turbulence, which is of order $a/\tau_{\rm K}$ [4], is replaced by a much larger relative velocity which characterises the relative motion of the fluid at different positions. This relative velocity may be parametrised by writing $\langle w \rangle \sim u_{\rm K} F(\mathrm{St}, \mathrm{Re})$, where $u_{\rm K} = (\epsilon\nu)^{1/4}$ is the velocity at the Kolmogorov scale, $F$ depends on the Stokes number, and the Reynolds number, Re. The collision rate is, therefore,

$$R_{\rm sling} = \frac{n_0 a^2 \eta}{\tau_{\rm K}} F(\mathrm{St}, \mathrm{Re}) \ . \tag{7}$$

The collision rate is the sum of contributions from collisions between particles which lie on the same branch of the phase-space manifold, giving rise to $R_{\rm adv}$, and collisions between particles on different branches, giving rise to $R_{\rm sling}$:

$$R = R_{\rm adv} + R_{\rm sling} \tag{8}$$

This decomposition, proposed in earlier works [9, 12, 25], rests on the assumption that the fraction of particles which give rise to preferential concentration, collide with a small relative velocity with respect to the fluid, whereas another fraction, evenly distributed in the fluid, moves with large relative velocity. The collisions due to these particles is described by the term $R_{\rm sling}$, with the analytic form in (7). When $\mathrm{St} \to 0$, the collision rate is well approximated by (5), but both terms can contribute to an enhanced collision rate as St increases. The principal question addressed by this paper is to determine which contribution dominates as St increases.

It is possible to consider the asymptotic forms for the function $F(\mathrm{St}, \mathrm{Re})$ in equation (7), in the limits of small and large Stokes numbers. In the limit as $\mathrm{St} \to 0$, we must have $F(\mathrm{St}, \mathrm{Re}) \to 0$, so that the limiting case (5) is recovered from (8). Considerations of model systems (described in [9]) suggest that $F$ has non-analytic behaviour

in this limit, such as $F(\mathrm{St},\mathrm{Re}) \sim \exp(-C/\mathrm{St})$, for some constant $C$: this is consistent with numerical results with the Navier-Stokes equations [26]. The asymptotic form of the function $F(\mathrm{St},\mathrm{Re})$ at large Stokes numbers has been considered by several authors. Abrahamson's theory is not valid for fully-developed turbulence, because it ignores the multiscale structure of the flow. A version which correctly accounts for the multiscale structure of turbulence was proposed by Völk *et al.* [27], using the Kolmogorov model for the structure of the flow. This theory suggests that $F(\mathrm{St},\infty) \sim \mathrm{St}^{1/2}$. A simpler and more general argument was proposed in [28]: in the inertial range, the relative velocity can only depend upon $\epsilon$ and $\tau_\mathrm{p}$, so that dimensional analysis mandates that $\langle w \rangle \sim \sqrt{\epsilon \tau_\mathrm{p}}$. Substituting for $\tau_\mathrm{p}$, we have a rate of collision at high Stokes number which is of the form (7) with $F(\mathrm{St},\infty) \sim K\sqrt{\mathrm{St}}$, where $K$ is a universal dimensionless constant. We emphasise that, because the preferential concentration effect is a consequence of nearby particles experiencing a corrrelated strain-rate, this effect makes no contribution to $R_\mathrm{sling}$. Equation (7) accounts for collisions between particles which have not experienced the same local environment, and the factor $g(2a)$ which occurs in (6) is therefore absent from (7).

We investigated the collision rate $R$ as a function of both $a$ and $\rho_\mathrm{p}/\rho_\mathrm{f}$. Our simulations used a pseudo-spectral code, fully dealiased, with grid size $384^3$. The flow is forced with a prescribed energy injection rate $\epsilon$ [29]. The Taylor microscale Reynolds number achieved in the steady state is $\mathrm{Re}_\lambda = 130$. Proper spatial resolution has been maintained, as can be judged from the product $k_\mathrm{max}\eta = 2$, where $\eta = (\nu^3/\epsilon)^{1/4}$ is the Kolmogorov scale, and $k_\mathrm{max}$ the largest wavenumber faithfully simulated. Particle trajectories were integrated by using the Velocity Verlet algorithm [30] and resorting to tri-cubic interpolation to evaluate the fluid velocity at the position of the particle. We detected collisions by using the algorithm described in [31]. Modifying the ratio $\rho_\mathrm{p}/\rho_\mathrm{f}$ at fixed value of the Stokes number is achieved by varying in the collision detection algorithm the radius of the particles, $a$, according to (2),(3) (so that $a \propto (\rho_\mathrm{p}/\rho_\mathrm{f})^{-1/2}$). In the range of parameters considered, $\rho_\mathrm{p}/\rho_\mathrm{f} > 250$ and $\mathrm{St} \leq 5$, the particle radii are at most $\approx \eta/3$, which ensures that (1) provides a very good description of the motion. We find that after a transient state of $\approx 5$ eddy turnover times, the collision rate becomes independent of time. The collision rates were determined by recording at the minimum $1.3 \times 10^4$ collisions when $\rho_\mathrm{p}/\rho_\mathrm{f} = 10^3$, accumulated (except in one case) over $\gtrsim 10$ eddy-turnover times.

The collision rate, $R$, determined numerically is plotted in Fig. 1. As explained earlier, we do not distinguish here between single and multiple collisions. In Fig. 1(a), $R$ is normalized by $n_0(2a)^2/\tau_\mathrm{K}$ and plotted as a function of St. The Saffman-Turner prediction, (5), implies that in the limit $St \to 0$, the quantity $R\tau_\mathrm{K}/(n_0(2a)^3)$ should become independent of the ratio $\rho_\mathrm{p}/\rho_\mathrm{f}$. Our own numerical results are only consistent with this prediction for

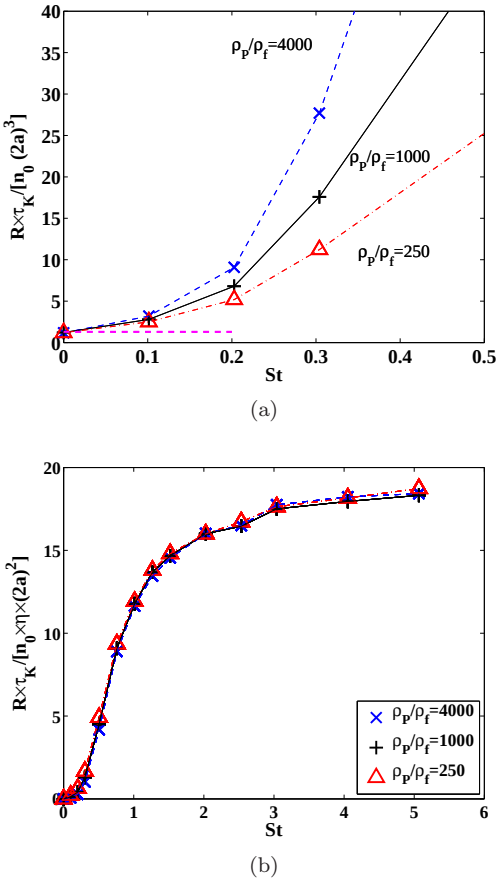


FIG. 1. The collision rate $R$ as a function of the Stokes number St and for the ratios of density $\rho_\mathrm{p}/\rho_\mathrm{f} = 250$, $10^3$ and $4.10^3$. The collision rate $R$ is normalized by $n_0(2a)^3/\tau_\mathrm{K}$ (a), and $n_0(2a)^2\eta/\tau_\mathrm{K}$ (b). The horizontal dashed line in (a) corresponds to the Saffman-Turner prediction.

small values of St. Fig. 1(b) shows that $R\tau_\mathrm{K}/(n_0 a^2 \eta)$ as a function of the Stokes number, does not depend much on $\rho_\mathrm{p}/\rho_\mathrm{f}$ for values of St larger than $\gtrsim 0.3$. This scaling is consistent with the sling/caustics collision mechanism, described by equation (7). We note that $F(St, Re)$ deduced from Fig. 1(b) does not fit the asymptotic form $F(\mathrm{St},\infty) = K\sqrt{\mathrm{St}}$ for large values of St. We ascribe this to the limited Reynolds number of our numerical simulations.

A clear illustration of the transition from the regime described by the Saffman-Turner prediction, (5), and the sling dominated regime, (7), is provided by Fig. 2 which shows the ratio between the values of $R$ computed at $\rho_\mathrm{p}/\rho_\mathrm{f} = 4000$ and 1000 (crosses) and $\rho_\mathrm{p}/\rho_\mathrm{f} = 1000$ and 250 (triangles). Whereas (5) predicts that these ratios should be 1/8, (7) predicts rather a ratio of 1/4. Fig. 2 shows that the ratios are extremely close to 1/4 for $St \gtrsim 0.5$, but approaches 1/8 for $\mathrm{St} \lesssim 0.3$.

Fig. 3 shows the function $g(2a)$, (which quantifies the importance of preferential concentration) in our simula-

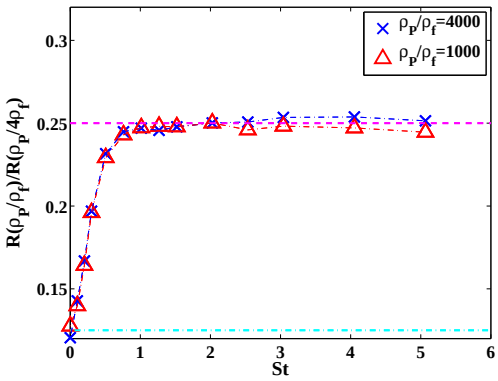


FIG. 2. The ratio between the collision rates $R$ corresponding to $\rho_{\rm p}/\rho_{\rm f} = 4000$ and 1000 (crosses) and $\rho_{\rm p}/\rho_{\rm f} = 1000$ and 250 (triangles), illustrating the crossover between the sling dominated regime for St $\gtrsim 0.5$, and the regime described by the Saffman-Turner theory for St $\lesssim 0.2$.

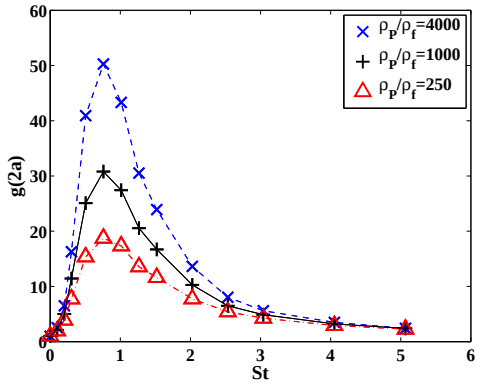


FIG. 3. The function $g$ that measures preferential concentration, computed for three values of $a$, corresponding to particles with a density $\rho_{\rm p}$ equal to $250\rho_{\rm f}$, $1000\rho_{\rm f}$ and $4000\rho_{\rm f}$, as indicated in the figures. The preferential concentration does not play a significant role for St $\gtrsim 5$

tions for the three different values of $\rho_{\rm p}/\rho_{\rm f}$. The strong enhancement of the concentration at the surface of a particle is not sufficient to make the advective collision rate (6) comparable to the sling collision rate, (7).

Further evidence for the importance of caustics comes from considering the probability density, $P(w|2a)$, of the radial relative velocity between two particles, $w \equiv \delta\mathbf{v}\cdot\delta\mathbf{r}/|\delta\mathbf{r}|$, conditioned on the fact that the two particles collide ( $|\delta\mathbf{r}| = 2a$ and $w \le 0$). Fig. 4 shows the cumulative PDF, $C(|w|)$, and the contribution of particles of velocity $w' < |w|$ to the flux [13], $C_\Phi(|w|)$:

$$C(|w|) = \int_0^{|w|} P(w'|2a)\ {\rm d}w'$$
$$C_\Phi(|w|) = \frac{\int_0^{|w|} P(w'|2a)\ w'\ {\rm d}w'}{\int_0^{\infty} P(w'|2a)\ w'\ {\rm d}w'} \qquad (9)$$

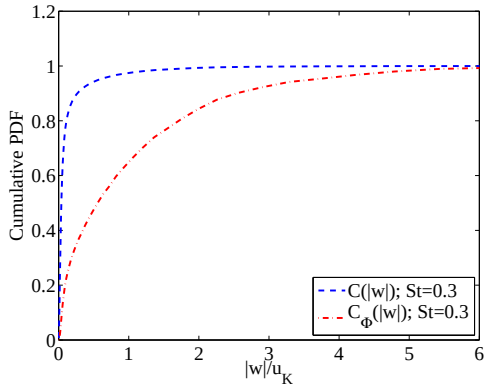


FIG. 4. The cumulative distribution of radial velocities of colliding particles, $C(|w|)$ (dashed line), and the cumulative distribution weighted by $|w|$, $C_\Phi(|w|)$ (dashed-dotted line), defined by Eq. (9). These describe the contribution to the collision rate due to particle pairs colliding with relative velocity less than $|w|$. While particles with a velocity larger than $u_{\rm K}$ are very few, they are responsible for a sizable fraction of the collision rate. The data shown corresponds to St = 0.3; $u_{\rm K}\times\tau_{\rm K}/(2a) \approx 27$, and $\rho_{\rm p}/\rho_{\rm f} = 1000$.

Even for values of the Stokes number as low as St = 0.3, $\sim 90\%$ of all particle pairs have a relative velocity difference less than $|w| \lesssim 8(2a)/\tau_{\rm K}$, but contribute only to $\sim 37\%$ of the collision rate. Fig. 4 therefore demonstrates that the contribution of the sling term is the prevalent effect responsible for the large increase of the collision rate, even at moderate Stokes numbers.

An alternative decomposition, originally proposed in [13], expresses the collision rate $R$ as a product in which the term $g(2a)$, which describes the local concentration enhancement around a particle, appears as an overall factor:

$$R = 4\pi(2a)^2 g(2a)\langle w\rangle_{\rm eff} \qquad (10)$$

This representation, which is exact for a suitable definition of $\langle w\rangle_{\rm eff}$, suggests that the preferential concentration and sling effects act together to enhance the collision rate. Figure 1(b) demonstrates that if this parametrisation of the collision rate is used, then the dependence of $g(2a)$ upon $\rho_{\rm p}/\rho_{\rm f}$ shown in figure 3 must be cancelled (for St $\ge 0.5$) by a reciprocal dependence of the collision velocity, $\langle w\rangle_{\rm eff}$. In fact, previous measurements [15, 32] of the dependence of $g(r)$ and of the average velocity difference as a function of $r$ suggest power law dependences, the exponents being such that the product $g(2a)\langle w\rangle_{\rm eff}$ is essentially constant for St $\gtrsim 0.5$. Our equations (6), (7) and (8) give a physically well-motivated theory which explains the data, and provide an explanation for this cancellation.

We conclude that in turbulent flows and at large values of $\rho_{\rm p}/\rho_{\rm f}$ (the case relevant to typical aerosols), the sling effect provides the dominant mechanism for the dramatically enhanced collision rate, for particles whose Stokes number exceeds $\sim 0.3$.

The authors acknowledge informative discussions with B. Mehlig, K. Gustavsson and L. Collins. AP and EL have been supported by the grant from A.N.R. 'TEC 2'. Computations were performed at the PSMN computing center at the Ecole Normale Supérieure de Lyon. MW and AP were supported by the EU COST action MP0806 'Particles in Turbulence'.

[1] R. A. Shaw, *Annu. Rev. Fluid Mech.* **35**, 183-227 (2003).
[2] V. S. Safranov, *Evolution of the protoplanetary cloud and formation of earth and planets*, *NASA Tech. Transl. F-677; Moscow, Nauka* (1969).
[3] S. Elghobashi, *Applied Scientific Research* **52**, 309 (1994).
[4] P. G. Saffman and J. S. Turner, *J. Fluid. Mech.* **1**, 16-30 (1956).
[5] M. R. Maxey, *J. Fluid Mech.*, **174**, 441, (1987).
[6] M. Wilkinson, B. Mehlig, S. Östlund and K. P. Duncan, *Phys. Fluids*, **19**, 113303, (2007).
[7] G. Falkovich, A. Fouxon and M. G. Stepanov, *Nature* **419**, 151-154 (2002).
[8] M. Wilkinson and B. Mehlig, *Europhys. Lett.* **71**, 186 (2005).
[9] M. Wilkinson, B. Mehlig and V. Bezuglyy, *Phys. Rev. Lett.* **97**, 048501 (2006).
[10] J. Abrahamson, *Chem. Eng. Sci.* **30**, 1371-1379 (1975).
[11] E. Meneguz and M. W. Reeks, *J. Fluid Mech.* **686**, 338-351 (2011).
[12] L. Ducasse and A. Pumir, *Phys. Rev.* **E 80**, 066312 (2009).
[13] S. Sundaram and L. R. Collins, *J. Fluid Mech.* **335**, 75 (1997).
[14] L.P. Wang, A. S. Wexler and Y. Zhou, *J. Fluid Mech.* **415**, 117 (2000).
[15] B. Rosa, H. Parishani, O. Ayala, W. W. Grabowski and L. P. Wang, *New J. Phys.* **15**, 045032 (2013).
[16] M. R. Maxey and J. J. Riley, *Phys. Fluids* **26**, 883 (1983)
[17] R. Gatignol, *J. Mec. Theor. Appl.*, **1**, 143 (1983).
[18] W. Grabowski and P. Vaillancourt, *J. Atmos. Sci.*, **56**, 1433-1436 (1999).
[19] M. Wilkinson, B. Mehlig and V. Uski, *Astrophys. J., Suppl.*, **176**, 484, (2008).
[20] W. C. Reade and L. R. Collins, *Phys. Fluids* , **12**, 2530, (2000).
[21] J. Sommerer and E. Ott, *Science*, **259**, 335, (1993).
[22] J. Bec, *Phys. Fluids*, **15**, L81-4, (2003).
[23] P. Grassberger and I. Procaccia, *Physica D*, **9**, 189-208, (1983).
[24] J. Bec, L. Biferale, M. Cencini, A. Lanotte, S. Musacchio, and F. Toschi, *Phys. Rev. Lett.*, **98**, 084502, (2007).
[25] K. Gustavsson and B. Mehlig, *Phys. Rev.* **E 84**, 045304 (2011).
[26] G. Falkovich and A. Pumir, *J. Atmos. Sci.* **64**, 4497-4505 (2007).
[27] H. J. Völk, F. C. Jones, G. E. Morfill, and S. Röser, *Astron. Atrophys.* , **85**, 316, (1980).
[28] B. Mehlig, V. Uski and M. Wilkinson, *Phys. Fluids* **19**, 098107 (2007).
[29] A. G. Lamorgese, D. A. Caughey and S. B. Pope, *Phys. Fluids* **17**, 015106 (2005).
[30] W. H. Press, S. A. Teukolsky, W. T. Vetterling and B. P. Flannery, *Numerical Recipes: the art of scientific computing*, New York, Cambridge University Press (2007).
[31] S. Sundaram and L. R. Collins, *J. Comput. Phys.* **124**, 337 (1996).
[32] J. Bec, L. Biferale, M. Cencini, A. S. Lanotte and F. Toschi, *J. Fluid Mech.* **646**, 527-536 (2010).